Universal Conductance Fluctuations of Light

Frank Scheffold and Georg Maret
Fakultät für Physik, Universität Konstanz, Postfach 5560, D-78457 Konstanz, Germany
(Received 4 September 1998)

We observed that laser light, multiply scattered through small samples of optically dense colloidal suspensions, builds up anomalous long range correlations in the transmission speckle pattern. The dynamic autocorrelation function of angular integrated light intensity has two contributions, $C_2(t)$ and $C_3(t)$, which decay on very different time scales. C_2 and C_3 are explained by onefold and twofold crossing, respectively, of multiple scattering paths, in quantitative agreement with theory. Our C_3 data provide the first evidence for the classical wave analog of universal electronic conductance fluctuations and pinpoint their physical origin as a macroscopic quantum-wave interference effect. [S0031-9007(98)07990-3]

PACS numbers: 42.25.Bs, 05.40.+j, 42.30.Ms

Electron transport in disordered metals and photon transport in random dielectrics have surprising similarities. Since the discovery [1,2] of coherent backscattering of light as the photonic analog of weak electron localization much experimental and theoretical work [3] has revealed that fundamental transport properties are governed by interference effects for both classical and quantum mechanical waves.

A most interesting example is the phenomenon of universal conductance fluctuations (UCF). In mesoscopic samples of disordered metals large fluctuations of the electronic conductance are observed as a function of applied magnetic field or, equivalently, the positions of the scattering impurities [4]. The magnetic field causes phase shifts of the electronic wave function along the scattering paths, as does a moving scatterer, and therefore changes the interference condition in the total scattered wave field generating a fluctuating conductance. The amplitude was found close to the natural conductance scale e^2/h (with elementary charge e and Planck's constant h) independent of material and sample dimensions. These experiments require mesoscopic samples and low temperatures in order to suppress inelastic scattering which destroys phase coherence. Lasers, on the other hand, are strong sources of classical waves with coherence lengths much larger than macroscopic sample sizes. In addition, while electron-electron interaction adds substantial complexity to UCF, photon-photon interaction is negligible, and moreover light scattering intrinsically provides much more detailed information on wave correlations and fluctuations than electronic conductance. Interference effects on wave transport can therefore be studied ideally using visible light diffusing in a turbid medium [5].

Both classical and electronic conductance fluctuations are described [6,7] in an appealing simple physical picture as further outlined below: Interferences between waves scattered along independent paths give rise to short range angular fluctuations (C_1), in optics known as speckles. One crossing of paths generates correlations of all output speckle spots (C_2) while two crossings cause UCF (C_3). Long range C_2 correlations in transmission speckles where observed as a function of frequency shift [8,9] and dynamic correlation time [10]. However, no experimental observation of UCF of any classical waves has been reported yet. In this Letter we present first evidence of optical UCF, which occur in the transmission of visible light through highly turbid colloidal suspensions. Our measurements of the time dependent autocorrelation function $C_3(t)$ of the transmitted intensity are in excellent quantitative agreement with theoretical predictions using experimental parameters as determined independently from measurements of classical $C_1(t)$ and long ranged $C_2(t)$ speckle correlations.

The electronic conductance G of a disordered medium can be described by Landauer's formula $G \equiv \alpha \sum_{a,b} \langle T_{ab} \rangle$ as a sum over the transmission probabilities T_{ab} of a single incoming wave mode a into an outgoing mode b, with $\alpha = e^2/h$ [7]. This description reduces the quantum transport of electrons to the simpler problem of scalar wave transport. To compare classical and quantum transport it is useful to introduce the *dimensionless conductance* $g = G/\alpha = \sum_{a,b} \langle T_{ab} \rangle$. The number N of modes, or *transport channels*, in a sample with cylindrical waveguide geometry of length L and diameter D is determined by D, $N = (kD)^2/4$ [11] where $k = 2\pi/\lambda$ denotes the wave vector of the propagating fields. Summing up the average transmission probability in diffusive transport through individual channels gives *Ohm's law*: $g = Nl^*/L$ [7]. Here, the only material-specific quantity is the transport mean free path l^*. Fluctuations are characterized by $\langle (\delta G)^2 \rangle$ which is the sum over the four field correlation function $C_{a,b,a',b'} = \langle \delta T_{a,b} \delta T_{a',b'} \rangle$ between two input and two output modes [7]: $\langle (\delta G)^2 \rangle = \alpha^2 \sum_{a,b,a',b'} C_{a,b,a',b'}$. In light scattering experiments, contrary to electronic systems, $C_{a,b,a',b'}$ can be measured directly since the incident and scattered wave vectors (defining incoming and outgoing modes) can be chosen at will. Using diagrammatic techniques Feng *et al.* [6] showed that the autocorrelation

 0031-9007/98/81(26)/5800(4)$15.00

function $C_{a,b,a',b'} = \langle I(0)I(t)\rangle/\langle I(0)\rangle^2 - 1$ of the scattered intensity has three contributions,

$$C_{a,b,a',b'}(t) = C_1(t) + \frac{1}{g} C_2(t) + \frac{1}{g^2} C_3(t). \quad (1)$$

t is a parameter, e.g., frequency shift of the incident wave field or correlation time in a dynamic system, which introduces phase shifts between the multiply scattered fields. In our experiments on colloidal suspensions these phases—and hence the speckle spots—fluctuate because of Brownian motion of scattering particles. When describing the diffuse propagation of classical waves in the physically more intuitive picture of a random walk of scattered waves the three terms of $C(t)$ are simply identified as respective contributions of zero, one or two crossing events of light paths [7,10]. Then, it is easy to show that $1/g$ equals the probability of two light paths to intersect once somewhere inside the medium.

Since $g \gg 1$ in typical optical experiments, most scattering paths do not cross and $C_1(t)$ describes the intensity fluctuations of one output mode b when illuminated by a single incoming mode a (Fig. 1). The intensity fluctuations contributing to $C_1(t)$ are of order unity. They give rise to the well known granular pattern of uncorrelated speckle spots. In the far field individual speckle spots have an angular width $\approx \lambda/D$ and can be directly identified as the N modes transmitted by the waveguide. Because of the randomness of paths, fields scattered along different nonintersecting paths are uncorrelated and their mutual interference contributions to $C_1(t)$ average to zero. Hence $C_1(t)$ is determined by the autocorrelation of fields scattered along individual paths, where the total phase shift along a single path is, on average, directly proportional to the length of the path [12]. $C_1(t)$ is a rapidly decaying function,

$$C_1(t, L) \simeq \exp\left[-2\left(\frac{L}{l^*}\right)^2 \frac{t}{\tau_0}\right], \quad (2)$$

$\tau_0 = (D_s k^2)^{-1}$ being the single scattering decay time for particles with diffusion constant D_s. Measurements of $C_1(t, L)$ are widely exploited in *diffusing wave spectroscopy* (DWS) which has become a powerful tool to study dynamics of colloids, emulsions, and other turbid soft matter [12,13].

$C_2(t)$ describes correlations of all outgoing modes for single mode illumination. Contributions to the decay of $C_2(t)$ originate from path sections before the crossing of two paths (Fig. 1) since behind the crossing the scattered fields stay completely time correlated along the remaining section of the path. This leads to a much slower and broader decay of $C_2(t)$ because the *active* path sections are shorter and more broadly distributed [14],

$$C_2(t, L) \simeq \frac{3}{2u}\left(\coth u - \frac{u}{\sinh^2 u}\right) \approx \frac{1}{L}\int_o^L C_1(t, z)dz, \quad (3)$$

with $u = L/l^*\sqrt{6t/\tau_0}$. In addition, this contribution does not depend on the angle of observation (b, b'). Hence, if a particular speckle spot is brighter than average all other speckle spots tend to be brighter as well. In a cylindrical waveguide the crossing probability $1/g$ is independent on depth z. Approximating the contributions of the phase shifts occurring before the crossing event at depth z by $C_1(t, z)$ leads to the right-hand side of Eq. (3). Numerical calculations of the integral reveal perfect agreement in shape and less than 5% difference in decay time between both expressions. This shows that within the random walk picture Eq. (3) gives an accurate approximation to the exact theoretical expression [14] for $C_2(t, L)$.

$C_3(t)$ describes correlations of all incoming modes with all outgoing modes. This term, of amplitude $1/g^2$, is the optical analog of UCF of a mesoscopic wire. The active path sections contributing to a decay of $C_3(t)$ are located between the two crossing events (Fig. 1) resulting in a further broadening and slowing down compared to $C_2(t)$, as seen by the integral approximation discussed above,

$$C_3(t) \approx \frac{1}{L}\int_o^L C_2(t, z)dz. \quad (4)$$

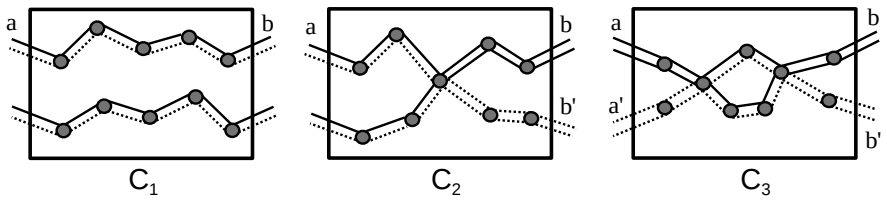

FIG. 1. The physics of conductance fluctuations: (C_1) Nonintersecting scattering paths give rise to short range temporal and angular speckle fluctuations because of scatterers motion. (Solid line) wave fields at correlation time $t = 0$ and (dashed line) phase shifted wave fields at $t > 0$ scattered along the *same* sequence of scatterers. There are no correlations between fields scattered along different paths. (C_2) One crossing of scattering paths builds up correlations between different paths. Temporal decorrelation like in (C_1) occurs along the *active* section of the paths located in front of the crossing event, while after the crossing the fields remain totally correlated (no mutual phase shifts) at all t and all output directions (b, b'). (C_3) Twofold crossings generate universal conductance fluctuations. t-dependent phase shifts occur only between the crossing events; the intensity fluctuations are therefore insensitive to input (a, a') and output (b, b') directions.

$C_3(t)$ is insensitive to input and output directions highlighting the analogy to the electronic case. In electronic UCF phase shifts leading to magnetic field induced fluctuations are proportional to the change of flux through the area bounded by the two active path sections.

Samples were prepared from commercial colloidal TiO_2 in water as described in Ref. [10] but using pH 6. After stabilization with polyacrylic acid and several filtering steps down to 1.2 μm pore size the suspension was found rather monodisperse with average particle diameter $d \simeq 290$ nm and variance $(\delta d)^2/d^2 \simeq 0.15$, determined from cumulant analysis of the time autocorrelation function of single scattered light intensity. Concentration was 7% $\pm$ 1% by volume. Using a cell of known thickness ($L = 100$ μm) we found from DWS in transmission [Eq. (2)] $l^* = 1.35 \pm 0.1$ μm ($\tau_0 \simeq 3$ ms) [12]. The setup (Fig. 2) to measure UCF of light was designed in analogy to a mesoscopic wire in two lead configuration. A cylindrical pinhole (laser drilled in a disk shaped stainless steel foil of thickness $L = 13$ μm) was embedded in the suspension providing a liquid reservoir on both sides of the sample. The thickness of both layers L_1, L_2 sealed by glass windows was varied using different spacers. The sample was illuminated with a laser beam ($\lambda = 514.5$ nm) focused down to 150–200 μm beam diameter at intensities <100 mW. We performed measurements of the time autocorrelation function of the *angular integrated* transmitted intensity collected with a thick multimode fiber. Multiple runs of typically 500 $\times$ 3 sec were carried out at photon count rates of 500–2000 kHz. In this geometry the contribution $C_1(t)$ is time independent due to the angular averaging of the outgoing light over many speckle spots. The prelayer of variable thickness allowed us to separate $C_2(t)$ and $C_3(t)$ in the time domain: The active path sections of $C_2(t)$ are located before the (single) crossing events which occur almost exclusively within the pinhole. A sufficiently thick prelayer L_1 therefore leads to a rapid decay of $C_2(t)$ very similar to $C_1(t)$: $C_2'(t) \simeq C_1(t, L_1)$ for $L_1 \gg L$, as seen by replacing the integration limits in Eq. (3) by $[L_1, L_1 + L]$. On the other hand, according to Eq. (4), $C_3(t)$ should decay algebraically independent of the thickness of both layers L_1 and L_2 since the two crossing events occur essentially only within the pinhole. In this way $C_3(t)$ is measured at times where $C_2'(t)$ has already decayed. Physically the colloidal prelayer scrambles the incoming modes very rapidly thereby creating an effective multimode illumination of the pinhole on the time scales of interest for $C_3(t)$. We characterized the setup by measuring $C_2'(t)$ for different pinhole sizes using moderately thick surrounding layers ($L_1, L_2 \approx 50$ μm). The inset of Fig. 3a shows the g values determined from the amplitude of $C_2'(t)$. The results are in excellent agreement with theoretical predictions [15,16]. It is readily seen that due to the quadratic dependence of g on D the amplitude of $C_3(t)$ is very small ($1/g^2 < 10^{-5}$) for all pinhole sizes except for the smallest one $D = 4 \pm 0.5$ μm.

To achieve an effective separation of time scales between $C_2'(t)$ and $C_3(t)$ we used a prelayer thickness $L_1 \approx 100$ μm. To increase transmission, we replaced the colloidal suspension in (L_2) by pure water. Because of the

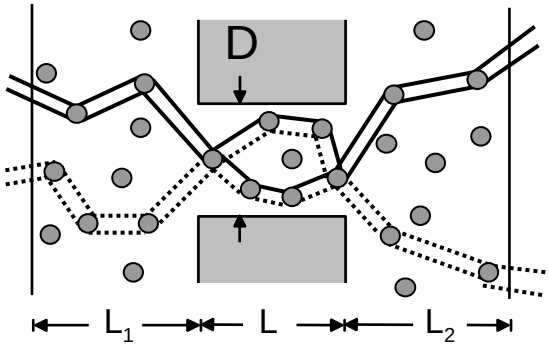

FIG. 2. Sketch of the experimental setup. A small cylindrical pinhole sandwiched between two layers is filled with a turbid colloidal suspension. Photon paths which cross twice inside the pinhole give rise to UCF.

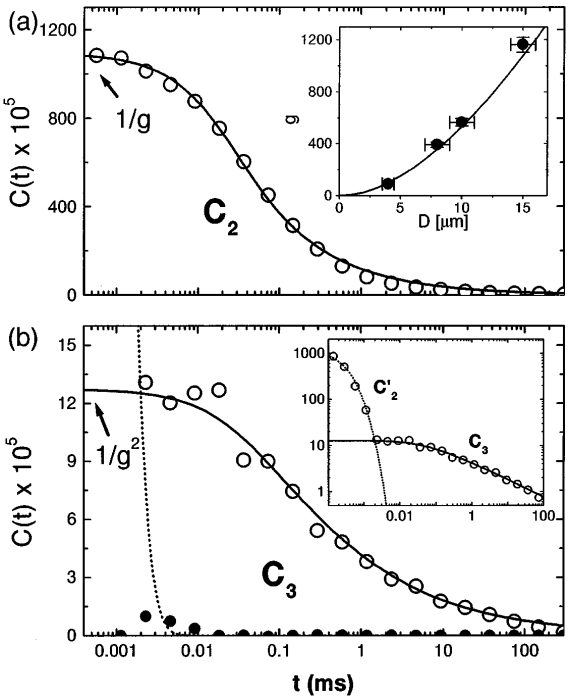

FIG. 3. (a) Inset: Dimensionless conductance g determined from the amplitude of $C_2'(t)$ measurements as a function of the pinhole diameter D. Solid line: theoretical prediction [16] with no adjustable parameter. Main figure: (○) $C_2(t)$ correlation function for the smallest pinhole $D = 4$ μm. Solid line: best fit by Eq. (3) with $g = 91, L = 13.1 \pm 1.3$ μm. (b) Universal conductance fluctuations $C_3(t)$ in comparison with $C_2'(t)$. For $t > 2 \times 10^{-3}$ ms, $C_2'(t)$ (dotted line) has decayed and $C_3(t)$ clearly shows up. Solid line: Theory [Eq. (4)] using $g = 89, L = 13.1$ μm. (●) Noise correlation function of the laser (no sample). Inset: log-log plot of the same data set.

absence of scattering in L_2 we were now able to measure the full $C_2(t)$ correlation function [Eq. (3)] of a cylindrical waveguide by illuminating the sample from the L_2 side. This provides additional information about the dynamics of the particles inside the pinhole which is difficult to obtain otherwise. The measured correlation function is shown in Fig. 3a. Since we expect $g = 98 \pm 23$ from theory for the pinhole foil thickness $L = 13$ μm [16], it is in excellent agreement with the theoretical prediction in amplitude, shape, and characteristic decay time. These results demonstrate that the dynamics of the particles inside the pinhole are largely unaffected by the lateral confinement, that the distribution of path lengths is not significantly altered by residual absorption at the pinhole walls, and that the finite values for d and l^* in relation to D are not important. Note that these measurements of g and $C_2(t)$ fully characterize the system.

In order to measure UCF we used the *identical* sample ($D = 4$ μm) which was now simply illuminated from the opposite side (L_1). As seen in Fig. 3b, the contribution of $C_2'(t)$ now decays very fast. For longer correlation times we observe $C_3(t)$ which decays over more than four decades in time. The value of the dimensionless conductance determined from the amplitude of $C_3(t)$, $g \simeq 89 \pm 5$ is found in good agreement with the value obtained from the $C_2(t)$ measurement ($g \simeq 91 \pm 4$). Equally good agreement is found by comparing the shape of the $C_3(t)$ correlation function with the theoretical curve [Eq. (4)] without any adjustable parameter.

In conclusion, our multiple light scattering experiments on very small samples of concentrated colloidal suspensions provide first evidence for universal conductance fluctuations in the transmission of classical waves. We have shown that the use of coherent laser sources combined with accurate time correlation techniques allows one to study very precisely the higher order correlation functions $C_2(t)$ and $C_3(t)$. Our data provide a complete picture of the microscopic origin of UCF in disordered conductors in general. We demonstrate that the (quantum) wave interference can be quantitatively described by the simple model of diffusing waves crossing at locations inside the sample where the lateral confinement is high. Like weak and strong Anderson localization, UCF are a direct consequence of wave interference effects on a macroscopic scale. These interference corrections increase with randomness resulting in the breakdown of classical transport theory.

Early discussions with P. E. Wolf and the late S. Feng are kindly acknowledged.

[1] P. W. Anderson, Philos. Mag. **52**, 505 (1985); S. John, Phys. Rev. B **31**, 304 (1985).
[2] M. P. Van Albada and A. Lagendjik, Phys. Rev. Lett. **55**, 2692 (1985); P. E. Wolf and G. Maret, Phys. Rev. Lett. **55**, 2696 (1985).
[3] P. Sheng, *Introduction to Wave Scattering, Localization, and Mesoscopic Phenomena* (Academic Press, Boston, 1995).
[4] C. P. Umbach *et al.*, Phys. Rev. B **30**, 4048 (1984); R. A. Webb *et al.*, Phys. Rev. Lett. **54**, 2696 (1985).
[5] Electromagnetic vector wave propagation in turbid media ($L \gg l^*$) can be described by scalar wave approximation since the memory of incident polarization is lost over about 1 l^*.
[6] S. Feng, C. Kane, P. A. Lee, and A. D. Stone, Phys. Rev. Lett. **61**, 834 (1988).
[7] S. Feng and P. Lee, Science **251**, 633 (1991).
[8] M. P. van Albada, J. F. de Boer, and A. Lagendijk, Phys. Rev. Lett. **64**, 2787 (1990); J. F. de Boer, M. P. van Albada, and A. Lagendijk, Phys. Rev. B **45**, 658 (1992).
[9] A. Z. Genack, N. Garcia, and W. Polkosnik, Phys. Rev. Lett. **65**, 2129 (1990).
[10] F. Scheffold, W. Härtl, G. Maret, and E. Matijevic, Phys. Rev. B **56**, 10 942 (1997).
[11] This differs by a factor of 2 from the original expression [6] for scalar waves due to the two polarization states of electromagnetic waves [8].
[12] G. Maret and P. E. Wolf, Z. Phys. B **65**, 409 (1987); D. J. Pine, D. A. Weitz, P. M. Chaikin, and E. Herbolzheimer, Phys. Rev. Lett. **60**, 1134 (1988); D. A. Weitz and D. J. Pine, in *Dynamic Light Scattering*, edited by W. Brown (Oxford University Press, New York, 1993), pp. 652–720.
[13] G. Maret, Curr. Opin. Coll. Int. Sci. **2**, 251–257 (1997).
[14] R. Berkovits and S. Feng, Phys. Rep. **238**, 135 (1994).
[15] R. Pnini and B. Shapiro, Phys. Rev. B **39**, 6986 (1989).
[16] Small deviations from a cylindrical waveguide are due to contributions outside the pinhole where the effective lateral confinement of the photon cloud spreads out linearly. This is taken into account by introducing an effective length of the pinhole $L + 3/8D$ [15].